SIAM J. NUMER. ANAL.
Vol. 53, No. 2, pp. 874–894

NONCONFORMING FEMs FOR AN OPTIMAL DESIGN PROBLEM*

C. CARSTENSEN† AND D. J. LIU‡

Abstract. Some optimal design problems in topology optimization eventually lead to a degenerate convex minimization problem $E(v) := \int_\Omega W(\nabla v)dx - \int_\Omega f\,v\,dx$ for $v \in H_0^1(\Omega)$ with possibly multiple minimizers u, but with a unique stress $\sigma := DW(\nabla u)$. This paper proposes the discrete Raviart–Thomas mixed finite element method (dRT-MFEM) and establishes its equivalence with the Crouzeix–Raviart nonconforming finite element method. The convergence analysis combines the a priori convergence rate of the conforming FEM with the efficient a posterior error control of MFEM. Numerical experiments provide empirical evidence that the proposed dRT-MFEM overcomes the reliability-efficiency gap for the first time.

Key words. finite element method, nonconforming, Crouzeix–Raviart, Raviart–Thomas, optimal design problem, reliability-efficiency gap, dual energy, two-sided energy estimates

AMS subject classifications. 65N12, 65N30, 65Y20

DOI. 10.1137/130927103

1. Introduction.

The optimal design of two materials with prescribed amounts but unknown position to fill a given domain for a maximal torsion stiffness is one model problem in topology optimization [17]. The mathematical modeling leads to the degenerate convex minimization problem with energy

$$E(v) := \int_\Omega \psi(|\nabla v|)dx - F(v) \qquad \text{for } v \in V := H_0^1(\Omega). \tag{1.1}$$

Here and throughout this paper, $F(v) := \int_\Omega f v\,dx$ is defined for a given datum $f \in L^2(\Omega)$ and the energy function $\psi : [0,+\infty) \to \mathbb{R}$ is defined, for given parameters $0 < t_1 < t_2$ and $0 < \mu_1 < \mu_2$ with $t_1\mu_2 = t_2\mu_1$, by $\psi(0) := 0$ and its derivative

$$\psi'(t) := \begin{cases} \mu_2 t & \text{for } 0 \le t \le t_1, \\ t_1\mu_2 = t_2\mu_1 & \text{for } t_1 \le t \le t_2, \\ \mu_1 t & \text{for } t \ge t_2. \end{cases} \tag{1.2}$$

The energy density $W : \mathbb{R}^2 \to \mathbb{R}$ reads $W(A) := \psi(|A|)$ with the derivative $DW(A) = \psi'(|A|)A/|A|$ for all $A \in \mathbb{R}^2 \setminus \{0\}$ and has the dual function $W^*(A) := \psi^*(|A|)$ with

$$\psi^*(t) := \begin{cases} t^2/(2\mu_2) & \text{for } t \le t_1\mu_2, \\ t^2/(2\mu_1) - \mu_1 t_2(t_2 - t_1)/2 & \text{for } t \ge t_1\mu_2. \end{cases} \tag{1.3}$$

Numerous works [19, 18, 17, 15, 4, 8] have been devoted to the mathematical analysis and numerical computation of the minimization of (1.1). The conforming

*Received by the editors July 1, 2013; accepted for publication (in revised form) December 15, 2014; published electronically March 31, 2015.
http://www.siam.org/journals/sinum/53-2/92710.html

†Institut für Mathematik, Humboldt-Universität zu Berlin, D-10099 Berlin, Germany, and Department of CSE, Yonsei University, 120749 Seoul, Korea (cc@math.hu-berlin.de). The research of this author was supported by the German Research Foundation (DFG) under Research Group 797, Analysis and Computation of Microstructure in Finite Plasticity, and DGF Research Group Multiplast.

‡Corresponding author. Department of Mathematics, College of Sciences, Shanghai University, Shanghai 200444, People's Republic of China (liudj@shu.edu.cn). The research of this author was supported by the National Natural Science Foundation of China (11001168, 61201113) and the Shanghai Municipal Education Commission Project.

finite element method (CFEM) in the primal form is analyzed in [4, 18, 16] with a priori and a posteriori error estimates [14]. Even for some larger class of convex energy functionals, the stress field $\sigma := DW(\nabla u)$ is unique and locally smooth $\sigma \in H^1_{loc}(\Omega;\mathbb{R}^2)$ [15] and satisfies $\sigma \in H^{1/2-\delta}(\Omega;\mathbb{R}^2)$ with any $0 < \delta < 1/2$ for a general Lipschitz domain Ω [21]. However, the guaranteed smoothness of the stress σ does not guarantee any convergence rates for the CFEM. The smoothness of σ motivated the mixed FEM (MFEM) in the dual formulation with a priori and a posteriori error estimates in [13]. That version of [13] is costly because of the exact integral quadrature of the affine functions applied to the continuous but nonsmooth energy density W^* with an extra regularization.

This paper proposes some simplified MFEM with one-point numerical quadrature and explores some surprising advantages of the novel discrete Raviart–Thomas mixed finite element method (dRT-MFEM). First, the dRT-MFEM is equivalent to the Crouzeix–Raviart nonconforming first-order finite element method (CR-NCFEM). The nondifferentiability of W^* enforced a regularization [13], while the new equivalence to CR-NCFEM for the primal problem with the smooth energy density W leads to a novel advantageous numerical scheme. This generalizes the Marini representation [2, 23] and Arbogast and Chen [1] from linear and general variable coefficients elliptic PDEs to nonlinear convex minimization problems. Second, the convergence analysis of dRT-MFEM (CR-NCFEM) combines the best aspects of the primal and dual formulation, namely, the a priori convergence rate of CFEM with the efficient a posteriori error control of MFEM. For the first time, this leads to some optimal convergence rates with effective a posteriori error control which overcomes the reliability-efficiency gap. The reliability-efficiency gap arises in degenerate minimization problems and systematically leads to efficient error estimates, which are not known to be reliable, and to reliable error estimates, which are guaranteed but not efficient [14].

The remaining parts of this paper are organized as follows. Section 2 introduces the precise notation and states the four finite element methods for the optimal design problem. Section 3 establishes the equivalence result of dRT-MFEM and CR-NCFEM. A priori and a posteriori error estimates of CR-NCFEM, RT-MFEM, and dRT-MFEM follow in sections 4, 5, and 6, respectively. Some numerical experiments conclude the paper in section 7 with empirical evidence of the superiority of the new CR-NCFEM also for adaptive mesh-refinement.

Standard notation applies throughout this paper to Lebesgue and Sobolev spaces $L^2(\Omega)$, $H^s(\Omega)$, and $H(\mathrm{div},\Omega)$, as well as to the associated norms $\|\cdot\| := \|\cdot\|_{L^2(\Omega)}$, $|||\cdot||| := \|\nabla\cdot\|_{L^2(\Omega)}$, and $|||\cdot|||_{NC} := \|\nabla_{NC}\cdot\|_{L^2(\Omega)}$ with the piecewise gradient $\nabla_{NC}\cdot|_T := \nabla(\cdot|_T)$ for all T in a regular triangulation $\mathcal{T}$ of the polygonal Lipschitz domain Ω. The notation $A \lesssim B$ abbreviates $A \le C\,B$ with some generic constant $0 \le C < \infty$, which depends on the interior angles of the triangles but not their sizes. The notation is for two dimensions for brevity but the arguments immediately carry over to higher space dimensions.

2. Four FEMs for optimal design problem.

2.1. Triangulations. Let $\mathcal{T}$ be a regular triangulation of the simply connected bounded Lipschitz domain $\Omega \subseteq \mathbb{R}^2$ with polygonal boundary $\partial\Omega$ into closed triangles. That is, the intersection of two distinct and nondisjoint triangles is either a common node or a common edge. Let $\mathcal{E}$ denote the set of all edges and let $\mathcal{E}(\Omega)$ (resp., $\mathcal{E}(\partial\Omega)$) denote the set of all interior (resp., boundary) edges, $\mathcal{N}$ denote the set of vertices, and $\mathcal{N}(\Omega)$ (resp., $\mathcal{N}(\partial\Omega)$) denote the interior (resp., boundary) nodes. For any triangle $T \in \mathcal{T}$, set $h_T := \mathrm{diam}(T)$, let $\mathcal{E}(T)$ denote the set of three edges of T, and write

$h_E := \operatorname{diam}(E)$ for an edge $E \in \mathcal{E}(T)$. Let

$$\mathcal{P}_k(\mathcal{T}) = \{v_k : \Omega \to \mathbb{R} \mid \text{for all } T \in \mathcal{T}, v_k|_T \text{is a polynomial of total degree} \le k\}$$

denote the set of piecewise polynomials and let $h_\mathcal{T} \in \mathcal{P}_0(\mathcal{T})$ denote the $\mathcal{T}$ piecewise constant mesh size function with $h_\mathcal{T}|_T = h_T$ for all $T \in \mathcal{T}$ and the maximum $h_{\max} := \|h_\mathcal{T}\|_\infty$. Assume that $\mathcal{T}$ is shape-regular so that $h_T \approx h_E \approx |T|^{1/2}$ for all $E \in \mathcal{E}(T)$ and $T \in \mathcal{T}$.

Let $[\bullet]_E := \bullet|_{T_+} - \bullet|_{T_-}$ denote the jump across the common edge $E = \partial T_+ \cap \partial T_-$ with $T_+, T_- \in \mathcal{T}$ and unit normal ν_E pointing into T_-. Let $\Pi_0 : L^2(\Omega) \to \mathcal{P}_0(\mathcal{T})$ denote the L^2 projection onto $\mathcal{T}$ piecewise constant, i.e., $(\Pi_0 f)|_T = ⨍_T f dx$ for all $T \in \mathcal{T}$(the same notation Π_0 is also used for vectors and is understood componentwise), and let $\operatorname{osc}(f, \mathcal{T}) := \|h_\mathcal{T}(f - \Pi_0 f)\|$.

2.2. $\mathcal{P}_1$ conforming FEM. The $\mathcal{P}_1$ conforming finite element approximation u_C to (1.1) minimizes the energy E in the Courant finite element space $V_C(\mathcal{T}) := \mathcal{P}_1(\mathcal{T}) \cap V$, written

$$u_C \in \arg\min E(V_C(\mathcal{T})). \tag{2.1}$$

It is proved in [16] that the dual variable $\sigma_C := DW(\nabla u_C)$ is unique, while the discrete minimizers u_C from (2.1) exist and are (possibly) nonunique. A priori error and a posteriori error estimates have been analyzed in [4, 16],

$$\frac{1}{2\mu_2}\|\sigma - \sigma_C\| \le \min_{v_C \in V_C(\mathcal{T})} |||u - v_C|||.$$

Define $\eta_E := h_E^{1/2}|[\sigma_C]_E \cdot \nu_E|$ for the jump $[\sigma_C]_E \cdot \nu_E$ of the discrete stress σ_C in the normal direction ν_E across an interior edge E; then

$$\frac{1}{2\mu_2}\|\sigma - \sigma_C\|^2 + |E(u) - E(u_C)| \lesssim \sqrt{\sum_{E \in \mathcal{E}(\Omega)} \eta_E{}^2} + \operatorname{osc}(f, \mathcal{T}). \tag{2.2}$$

2.3. Crouzeix–Raviart nonconforming FEM. The Crouzeix–Raviart finite element space is defined as

$$CR_0^1(\mathcal{T}) := \{v_h \in \mathcal{P}_1(\mathcal{T}) \mid v_h \text{ is continuous at midpoints of interior edges and vanishes at midpoints of boundary edges}\}.$$

The NCFEM is based on $CR_0^1(\mathcal{T})$ and the nonconforming energy E_{NC} with $F_h(\bullet) := F \circ \Pi_0(\bullet) = \int_\Omega (\Pi_0 f) \bullet dx$ and

$$E_{NC}(v_{CR}) := \int_\Omega W(\nabla_{NC} v_{CR}) dx - F_h(v_{CR}) \qquad \text{for } v_{CR} \in CR_0^1(\mathcal{T}). \tag{2.3}$$

The Crouzeix–Raviart finite element approximation u_{CR} to (1.1) minimizes the energy E_{NC} in $CR_0^1(\mathcal{T})$, written

$$u_{CR} \in \arg\min E_{NC}(CR_0^1(\mathcal{T})). \tag{2.4}$$

The discrete stress $\sigma_{CR} := DW(\nabla_{NC} u_{CR})$ is unique, which will be proved in section 3, while an a priori and a posteriori error analysis follows in section 4.

2.4. Raviart–Thomas mixed FEM. The dual energy E^* is defined as

$$E^*(\tau) := -\int_\Omega W^*(\tau)dx \qquad \text{for } \tau \in L^2(\Omega;\mathbb{R}^2).$$

Here and throughout this paper, $W^*(A) := \sup_{B\in\mathbb{R}^2}(A\cdot B - W(B))$ denotes the dual of W [25] and reads $W^* = \psi^*(|\bullet|)$ with ψ^* from (1.3). The dual problem of (1.1) maximizes the energy E^* in

$$Q(f) := \{\tau \in H(\mathrm{div},\Omega) \mid f + \mathrm{div}(\tau) = 0 \text{ a.e. in } \Omega\},$$

written

$$\sigma = \arg\max E^*(Q(f)).$$

The maximizer σ is unique [13] and equals $\sigma = DW(\nabla u)$ for any minimizer u of E in V.

The mixed finite element scheme is based on the Raviart–Thomas finite element space

$$RT_0(\mathcal{T}) := \left\{p \in H(\mathrm{div},\Omega) \mid \text{for all } T\in\mathcal{T}, \exists a\in\mathbb{R}^2, b\in\mathbb{R}, \text{ for all } x\in T, p = a + bx\right\}$$

and the dual energy E^* in

$$Q(f,\mathcal{T}) := \{\tau_{RT} \in RT_0(\mathcal{T}) \mid \Pi_0 f + \mathrm{div}(\tau_{RT}) = 0 \text{ a.e. in } \Omega\}.$$

The Raviart–Thomas mixed finite element approximation σ_{RT} to the dual variable σ maximizes the energy E^* in $Q(f,\mathcal{T})$, written

$$\sigma_{RT} = \arg\max E^*(Q(f,\mathcal{T})). \tag{2.5}$$

The maximizer σ_{RT} is unique in $Q(f,\mathcal{T})$ [13]. An a priori and a posteriori error analysis follows in section 5.

2.5. Discrete Raviart–Thomas mixed FEM. The discrete Raviart–Thomas mixed finite element scheme is based on the one-point numerical quadrature with respect to the center of each triangle and the resulting discrete dual energy $E_d^* := E^* \circ \Pi_0$,

$$E_d^*(\tau_{RT}) = -\int_\Omega W^*(\Pi_0\tau_{RT})dx \qquad \text{for } \tau_{RT} \in Q(f,\mathcal{T}).$$

The discrete Raviart–Thomas mixed finite element approximation σ_{dRT} to the dual solution σ maximizes the energy E_d^* in $Q(f,\mathcal{T})$, written

$$\sigma_{dRT} = \arg\max E_d^*(Q(f,\mathcal{T})). \tag{2.6}$$

The strong convexity of W^* (see Lemma 3.4 below) shows that the maximizer σ_{dRT} is unique in $Q(f,\mathcal{T})$. An a priori and a posteriori error analysis follows in section 6.

3. CR-NCFEM is equal to dRT-MFEM. This section is devoted to the equivalence of CR-NCFEM from subsection 2.3 with dRT-MFEM from subsection 2.5 as a generalization of the Marini representation from the linear equations [1, 2, 23] to nonlinear convex minimization problems. The equivalence is expressed by the equivalence of σ_{dRT} with some postprocessing σ^*_{CR} of σ_{CR}, namely,

$$\sigma^*_{CR} := \sigma_{CR} - \frac{\Pi_0 f}{2}(\bullet - \mathrm{mid}(\mathcal{T})) \in \mathcal{P}_1(\mathcal{T};\mathbb{R}^2).$$

Here and throughout this paper, the piecewise affine function $\bullet - \mathrm{mid}(\mathcal{T}) \in \mathcal{P}_1(\mathcal{T})$ equals $x - \mathrm{mid}(T)$ at $x \in T \in \mathcal{T}$ with barycenter $\mathrm{mid}(T)$.

Theorem 3.1 (CR-NCFEM = dRT-MFEM with no discrete duality gap). *It holds that* $\sigma^*_{CR} = \sigma_{dRT}$ *and* $\max E^*_d(Q(f,\mathcal{T})) = \min E_{NC}(CR^1_0(\mathcal{T}))$.

The remaining parts of this section are devoted to the proof of Theorem 3.1 which is based on the following lemmas and the Crouzeix–Raviart interpolation operator $I_{NC} : V \to CR^1_0(\mathcal{T})$,

$$(I_{NC} v)(\mathrm{mid}(E)) := \fint_E v ds \quad \text{for all } E \in \mathcal{E}.$$

Lemma 3.2 ([12], property of the Crouzeix–Raviart interpolant). *Any* $v \in H^1(\Omega)$ *with its interpolation* $I_{NC} v$ *and the constant* $\kappa := \sqrt{j_{1,1}^{-2} + 1/18}$ *for the first positive root* $j_{1,1}$ *of the Bessel function of the first kind satisfy* $\nabla_{NC}(I_{NC} v) = \Pi_0 \nabla v$ *and*

$$\|v - I_{NC} v\| \le \kappa \|h_{\mathcal{T}}(1 - \Pi_0)\nabla v\| \le \kappa \|h_{\mathcal{T}} \nabla v\|.$$

Proof. This lemma is established with different constants κ in [12, 24]; the version here is in [10]. ∎

Lemma 3.3 (conforming $\mathcal{P}_3$ companion). *Given any* $v_{CR} \in CR^1_0(\mathcal{T})$*, there exists some* $v_3 \in \mathcal{P}_3(\mathcal{T}) \cap V$ *with* $v_{CR} = I_{NC} v_3$*,* $\Pi_0 v_{CR} = \Pi_0 v_3$*, and*

$$\|h_{\mathcal{T}}^{-1}(v_{CR} - v_3)\| + |||v_{CR} - v_3|||_{NC} \lesssim \min_{v \in V} |||v - v_{CR}|||_{NC}.$$

Proof. Given $v_{CR} \in CR^1_0(\mathcal{T})$, define some conforming approximation by the averaging of the possible values (also known as the precise representation)

$$v_1(z) := v^*_{CR}(z) := \lim_{\delta \to 0} \int_{B(z,\delta)} v_{CR} dx / |B(z,\delta)|$$

of the (possibly) discontinuous v_{CR} at any interior node $z \in \mathcal{N}(\Omega)$ with ball $B(z,\delta)$ of radius δ and area $|B(z,\delta)|$ around z. Linear interpolation of those values defines $v_1 \in \mathcal{P}_1(\mathcal{T}) \cap C_0(\Omega)$. The second step adds edge-bubble functions to v_1 and so defines $v_2 \in \mathcal{P}_2(\mathcal{T}) \cap C_0(\Omega)$, which equals v_1 at all nodes $\mathcal{N}$ and satisfies

$$\int_E v_{CR}\, ds = \int_E v_2\, ds \quad \text{for all } E \in \mathcal{E}(\Omega).$$

The third step adds the cubic bubble functions to v_2 such that the resulting function $v_3 \in \mathcal{P}_3(\mathcal{T}) \cap C_0(\Omega)$ equals v_2 along the edges and satisfies

$$\int_T v_{CR}\, dx = \int_T v_3\, dx \quad \text{for all } T \in \mathcal{T}.$$

Therefore, an integration by parts shows

$$\int_T \nabla v_{CR}\, dx = \int_T \nabla v_3\, dx \quad \text{for all } T \in \mathcal{T}.$$

The approximation and stability properties of v_1 have been studied in the context of preconditioners for NCFEM [5] (called enrichments therein). This and standard arguments also prove approximation properties and stability in the sense that

$$\|h_{\mathcal{T}}^{-1}(v_{CR} - v_3)\| + |||v_{CR} - v_3|||_{NC} \lesssim \min_{v\in V} |||v - v_{CR}|||_{NC}. \qquad \square$$

The subdifferential ∂W^* of W^* [25] is uniformly convex.

LEMMA 3.4. *Any $a, b \in \mathbb{R}^2$, $\alpha = DW(a)$, $\beta = DW(b)$ satisfy*

$$\frac{1}{2\mu_2}|\alpha - \beta|^2 \leq W(b) - W(a) - \alpha\cdot(b-a). \tag{3.1}$$

Any $\alpha, \beta \in \mathbb{R}^2$ and any $b \in \partial W^*(\beta)$ satisfy

$$\frac{1}{2\mu_2}|\alpha - \beta|^2 \leq W^*(\alpha) - W^*(\beta) - b\cdot(\alpha-\beta). \tag{3.2}$$

Proof. The paper [4, Proposition 4.2] proves (3.1), which is also known as convexity control of W. The duality in convex analysis shows that the relation $\alpha = DW(a)$ is equivalent to $W^*(\alpha) + W(a) = a\cdot\alpha$ [25, Thm 23.5]. This implies

$$W^*(\alpha) + W(a) = a\cdot\alpha \ \text{ and } \ W^*(\beta) + W(b) = b\cdot\beta.$$

The combination with (3.1) concludes the proof of (3.2). $\square$

LEMMA 3.5 (uniqueness of σ_{CR}). *The discrete stress σ_{CR} is unique and satisfies the discrete Euler–Lagrange equation in the sense that*

$$\int_\Omega \sigma_{CR}\cdot\nabla_{NC} v_{CR} dx = \int_\Omega (\Pi_0 f)\ v_{CR} dx \qquad \text{for } v_{CR} \in CR_0^1(\mathcal{T}).$$

Proof. For any $0 < \varepsilon < 1$ and any $v_{CR} \in CR_0^1(\mathcal{T})$, let

$$\delta_\varepsilon(x) := \frac{W(\nabla_{NC} u_{CR}(x) + \varepsilon\nabla_{NC} v_{CR}(x)) - W(\nabla_{NC} u_{CR}(x))}{\varepsilon} \quad \text{for all } x \in \Omega.$$

Since u_{CR} is a minimizer,

$$0 \leq \frac{E_{NC}(u_{CR} + \varepsilon v_{CR}) - E_{NC}(u_{CR})}{\varepsilon} = \int_\Omega \delta_\varepsilon(x) dx - F(v_{CR}). \tag{3.3}$$

Since W is smooth, it follows for almost every $x \in \Omega$ that

$$\begin{aligned} |\delta_\varepsilon(x)| &= \left|\frac{1}{\varepsilon}\int_0^1 \frac{DW(\nabla_{NC} u_{CR}(x) + \varepsilon s\nabla_{NC} v_{CR}(x))}{\partial s} ds\right| \\ &\leq \int_0^1 |DW(\nabla_{NC} u_{CR}(x) + \varepsilon s \nabla_{NC} v_{CR}(x))\cdot\nabla_{NC} v_{CR}(x)| ds. \end{aligned}$$

The formula $DW(A) = \psi'(|A|)A/|A|$ leads to

$$|DW(A)| \leq |\psi'(|A|)| \leq \mu_2 |A| \qquad \text{for all } A \in \mathbb{R}^2.$$

This and the Young inequality imply that

$$|\delta_\varepsilon(x)| \le \mu_2 \int_0^1 |\nabla_{NC} u_{CR}(x) + \varepsilon s \nabla_{NC} v_{CR}(x)|\ |\nabla_{NC} v_{CR}(x)| ds$$
$$\lesssim |\nabla_{NC} v_{CR}(x)|^2 + |\nabla_{NC} u_{CR}(x)|^2.$$

Lemmas 3.3 and 3.2 imply that $\int_\Omega (|\nabla_{NC} v_{CR}(x)|^2 + |\nabla_{NC} u_{CR}(x)|^2)\ dx$ exists. Hence the Lebesgue dominate convergence theorem guarantees

$$\lim_{\varepsilon\to 0} \int_\Omega \delta_\varepsilon(x) dx = \int_\Omega DW(\nabla_{NC} u_{CR}) \cdot \nabla_{NC} v_{CR} dx.$$

This and (3.3) imply

$$0 \le \int_\Omega DW(\nabla_{NC} u_{CR}) \cdot \nabla_{NC} v_{CR} dx - F(v_{CR}).$$

Since v_{CR} is arbitrary in $CR^1_0(\mathcal{T})$, this proves the asserted discrete Euler–Lagrange equation.

The remaining part of the proof analyzes the uniqueness of the stress $\sigma_{CR} = DW(\nabla_{NC} u_{CR})$. Let u_{CR}, $\tilde{u}_{CR}$ be two minimizers of E_{NC} in $CR^1_0(\mathcal{T})$ and set $\tilde{\sigma}_{CR} := DW(\nabla_{NC} \tilde{u}_{CR})$. The choice $b := \nabla_{NC} u_{CR}$, $a := \nabla_{NC} \tilde{u}_{CR}$, and $\alpha := \tilde{\sigma}_{CR}$ in Lemma 3.4 leads to

$$\frac{1}{2\mu_2} \|\sigma_{CR} - \tilde{\sigma}_{CR}\|^2$$
$$\le \int_\Omega W(\nabla_{NC} u_{CR}) dx - \int_\Omega W(\nabla_{NC} \tilde{u}_{CR}) dx - \int_\Omega \tilde{\sigma}_{CR} \cdot \nabla_{NC}(u_{CR} - \tilde{u}_{CR}) dx$$
$$= E_{NC}(u_{CR}) - E_{NC}(\tilde{u}_{CR}).$$

Since $u_{CR}, \tilde{u}_{CR} \in \arg\min E_{NC}(CR^1_0(\mathcal{T}))$, $E_{NC}(u_{CR}) = E_{NC}(\tilde{u}_{CR})$. Hence $\sigma_{CR} = \tilde{\sigma}_{CR}$. This concludes the proof. ∎

LEMMA 3.6. *It holds that* $\sigma^*_{CR} \in Q(f, \mathcal{T}) \subseteq H(\mathrm{div}, \Omega)$.

Proof. The proof does not really involve the nonlinearity and focuses rather on the discrete Euler–Lagrange equations and so is very close to the linear case [23]. Hence the proof is briefly outlined here only for completeness.

Given $\sigma_{CR} \in \mathcal{P}_0(\mathcal{T}; \mathbb{R}^2)$ and $E \in \mathcal{E}(\Omega)$ with surface measure $|E|$, let $[\sigma^*_{CR}]_E \cdot \nu_E$ denote the jump of the discrete normal stress $\sigma^*_{CR} \cdot \nu_E$ over E and let ψ_E be the edge-oriented basis functions of $CR^1_0(\mathcal{T})$ which satisfy $\psi_E|_{\mathrm{mid}(E)} = 1$ and $\psi_E|_{\mathrm{mid}(F)} = 0$ for any $F \in \mathcal{E} \setminus \{E\}$. ω_E denotes the union of the elements that share the edge E. A piecewise integration by parts shows

$$[\sigma^*_{CR}]_E \cdot \nu_E |E| = \int_E \psi_E [\sigma^*_{CR}]_E \cdot \nu_E ds$$
$$= \int_{\omega_E} \nabla_{NC} \psi_E \cdot \sigma^*_{CR} dx + \int_{\omega_E} \psi_E\ \mathrm{div}_{NC} \sigma^*_{CR} dx$$
$$= \int_{\omega_E} \nabla_{NC} \psi_E \cdot \sigma_{CR} dx - \int_{\omega_E} (\Pi_0 f)\ \psi_E dx = 0.$$

Since E is arbitrary in $\mathcal{E}(\Omega)$, the normal component of ν jump of σ^*_{CR} across any interior edge vanishes. This concludes the proof. ∎

Proof of Theorem 3.1. For any minimizer u_{CR} of (2.4), the duality relation $\sigma_{CR} = DW(\nabla_{NC} u_{CR})$ implies that $\nabla_{NC} u_{CR} \in \partial W^*(\sigma_{CR})$. The choice of $\alpha := \Pi_0 \sigma_{dRT}|_T = \sigma_{dRT}(\mathrm{mid}(T))$, $\beta := \Pi_0 \sigma^*_{CR} = \sigma_{CR}$, and $b := \nabla_{NC} u_{CR}$ in Lemma 3.4 leads to

$$\begin{aligned}&\frac{1}{2\mu_2}\|\Pi_0\sigma_{dRT} - \Pi_0\sigma^*_{CR}\|^2\\ &\quad\le E^*(\Pi_0\sigma^*_{CR}) - E^*(\Pi_0\sigma_{dRT}) - \int_\Omega \nabla_{NC} u_{CR}\cdot(\sigma_{dRT} - \sigma^*_{CR})dx.\end{aligned}$$

An integration by parts and Lemma 3.6 with $\sigma_{dRT} \in Q(f,\mathcal{T})$ show that the last term vanishes. This and $E^*_d := E^* \circ \Pi_0$ prove

$$\frac{1}{2\mu_2}\|\Pi_0(\sigma_{dRT} - \sigma^*_{CR})\|^2 \le E^*_d(\sigma^*_{CR}) - E^*_d(\sigma_{dRT}).$$

Since $\sigma_{dRT} \in \arg\max E^*_d(Q(f,\mathcal{T}))$ and $\sigma^*_{CR} \in Q(f,\mathcal{T})$, the upper bound is nonpositive. Hence, $\Pi_0\sigma_{dRT} = \sigma_{CR}$ and $E^*_d(\sigma^*_{CR}) = E^*_d(\sigma_{dRT})$.

The duality relation $\sigma_{CR} = DW(\nabla_{NC} u_{CR})$ with the minimizer u_{CR} of (2.4) is equivalent to

$$W^*(\sigma_{CR}) + W(\nabla_{NC} u_{CR}) = \sigma_{CR}\cdot\nabla_{NC} u_{CR}.$$

An integration of this reads

$$\int_\Omega W(\nabla_{NC} u_{CR})dx - \int_\Omega \sigma_{CR}\cdot\nabla_{NC} u_{CR}dx = -\int_\Omega W^*(\sigma_{CR})dx.$$

The definition of E_{NC} and Lemma 3.5 show that the left-hand side (LHS) equals $E_{NC}(u_{CR})$. Moreover,

$$-\int_\Omega W^*(\sigma_{CR})dx = -\int_\Omega W^*(\Pi_0\sigma_{dRT})dx = E^*_d(\sigma_{dRT}).$$

Hence, $E^*(\sigma_{CR}) = E^*_d(\sigma_{dRT}) = E_{NC}(u_{CR})$. This concludes the proof. ∎

4. Error analysis of CR-NCFEM.

4. Error analysis of CR-NCFEM. This section analyzes the error estimates of the CR-NCFEM.

4.1. A priori error analysis. The combination of the regularity [21] with the subsequent a priori error estimate of Theorem 4.1 guarantees that the convergence rate is as $h_{\max}^{1/2-\epsilon}$ for the energy difference $|E(u) - E_{NC}(u_{CR})|$ and as $h_{\max}^{1/4-\epsilon}$ for stress difference $\|\sigma - \sigma_{CR}\|$ in terms of the maximal mesh-size $h_{\max} = \|h_\mathcal{T}\|_\infty$ for any $0 < \epsilon < 1/4$.

THEOREM 4.1 (a priori error estimate). *The discrete stress σ_{CR} satisfies*

$$\begin{aligned}&\|\sigma - \sigma_{CR}\|^2 + |E(u) - E_{NC}(u_{CR})|\\ &\quad\lesssim \max\left\{\|h_\mathcal{T} f\|\;|||u - I_{NC}u|||,\ \left(\mathrm{osc}(f,\mathcal{T}) + \|\sigma - \Pi_0\sigma\|\right)\,|||u - u_{CR}|||_{NC}\right\}.\end{aligned}$$

Proof. The choice $a := \nabla_{NC} u_{CR}$, $b := \nabla u$, and $\alpha := \sigma_{CR}$ in Lemma 3.4 leads to

$$\frac{1}{2\mu_2}\|\sigma - \sigma_{CR}\|^2 + E_{NC}(u_{CR}) - E(u) \le F(u - u_{CR}) - \int_\Omega \sigma_{CR}\cdot\nabla_{NC}(u - u_{CR})dx.$$

Since $\sigma_{CR} \in \mathcal{P}_0(\mathcal{T};\mathbb{R}^2)$ and

$$\int_\Omega \sigma_{CR} \cdot \nabla u dx = \int_\Omega \sigma_{CR} \cdot \nabla_{NC} I_{NC} u dx = F(I_{NC} u).$$

Hence,

$$\frac{1}{2\mu_2}\|\sigma - \sigma_{CR}\|^2 + E_{NC}(u_{CR}) - E(u) \le F(u - I_{NC}u). \tag{4.1}$$

The choice $a := \nabla u$, $b := \nabla_{NC} u_{CR}$, and $\alpha := \sigma$ in Lemma 3.4 leads to

$$\begin{aligned}\frac{1}{2\mu_2}\|\sigma - \sigma_{CR}\|^2 + E(u) - E_{NC}(u_{CR}) &\le F(u_{CR} - u) - \int_\Omega \sigma \cdot \nabla_{NC}(u_{CR} - u) dx \\ &= F(u_{CR}) - \int_\Omega \sigma \cdot \nabla_{NC} u_{CR} dx.\end{aligned}$$

The conforming $\mathcal{P}_3$ companion $u_3 \in \mathcal{P}_3(\mathcal{T}) \cap V$ with $u_{CR} = I_{NC} u_3$ shows

$$\begin{aligned}-\int_\Omega \sigma \cdot \nabla_{NC} u_{CR} dx &= -\int_\Omega \sigma \cdot \nabla u_3 dx + \int_\Omega \sigma \cdot \nabla_{NC}(u_3 - I_{NC} u_3) dx \\ &= -F(u_3) + \int_\Omega (1 - \Pi_0)\sigma \cdot (1 - \Pi_0)\nabla u_3 dx.\end{aligned}$$

The combination of the preceding estimates results in

$$\begin{aligned}&\frac{1}{2\mu_2}\|\sigma - \sigma_{CR}\|^2 + E(u) - E_{NC}(u_{CR}) \\ &\quad\le F(I_{NC} u_3 - u_3) + \int_\Omega (1 - \Pi_0)\sigma \cdot (1 - \Pi_0)\nabla u_3 dx.\end{aligned} \tag{4.2}$$

The sum of (4.1)–(4.2) reads

$$\frac{1}{\mu_2}\|\sigma - \sigma_{CR}\|^2 \le F((1 - I_{NC})(u - u_3)) + \int_\Omega (1 - \Pi_0)\sigma \cdot (1 - \Pi_0)\nabla u_3 dx. \tag{4.3}$$

Moreover, (4.1)–(4.2) imply that

$$\begin{aligned}&\frac{1}{2\mu_2}\|\sigma - \sigma_{CR}\|^2 + |E(u) - E_{NC}(u_{CR})| \\ &\quad\le \max\left\{F(u - I_{NC}u),\ F(I_{NC} u_3 - u_3) + \int_\Omega (1 - \Pi_0)\sigma \cdot (1 - \Pi_0)\nabla u_3 dx\right\}.\end{aligned} \tag{4.4}$$

The Cauchy–Schwarz inequality and Lemma 3.2 prove

$$\begin{aligned}F(I_{NC} u_3 - u_3) &\le \kappa \operatorname{osc}(f, \mathcal{T})\ |||u_3 - I_{NC} u_3|||_{NC}, \\ F(u - I_{NC} u) &\le \kappa \|h_{\mathcal{T}} f\|\ |||u - I_{NC} u|||_{NC}.\end{aligned}$$

This and Lemma 3.3 prove the assertion. ∎

4.2. A posteriori error analysis. This subsection is devoted to an a posteriori error analysis of the CR-NCFEM.

THEOREM 4.2 (a posteriori error estimate). *The discrete stress σ_{CR} and the constant $C_1 := 2\kappa C_F\|f\|/\mu_1$ satisfy*

$$\begin{aligned}\frac{1}{4\mu_2}\|\sigma - \sigma_{CR}\|^2 + |E(u) - E_{NC}(u_{CR})| \\ \leq \max\left\{F(u_{CR} - u_3) + \mu_2|||u_{CR} - u_3|||_{NC}^2, C_1\|h_{\mathcal{T}} f\|\right\}.\end{aligned} \tag{4.5}$$

The proof of Theorem 4.2 is based on the boundness of minimizers. Recall that any $v \in V$ satisfies the Friedrichs inequality

$$\|v\| \leq C_F|||v|||$$

with $C_F \leq \text{width}(\Omega)/\pi$. Any $v_{CR} \in CR_0^1(\mathcal{T})$ satisfies the discrete Friedrichs inequality [6, p. 301] with some constant $C_{dF} \approx 1$:

$$\|v_{CR}\| \leq C_{dF}|||v_{CR}|||_{NC}.$$

Proof of Theorem 4.2. The energy density W satisfies some two-sided growth condition in the sense that

$$\frac{\mu_1}{2}|A|^2 \leq W(A) \leq \frac{\mu_2}{2}|A|^2 \quad \text{for all } A \in \mathbb{R}^2. \tag{4.6}$$

The Friedrichs inequality shows that

$$\frac{\mu_1}{2}|||u|||^2 - C_F\|f\|\ |||u||| \leq E(u).$$

Since $E(u) \leq E(0) = 0$, this implies

$$|||u||| \leq \frac{2C_F}{\mu_1}\|f\|. \tag{4.7}$$

In the same way (with the discrete Friedrichs inequality rather than the original one),

$$|||u_{CR}|||_{NC} \leq \frac{2C_{dF}}{\mu_1}\|f\|. \tag{4.8}$$

Lemma 3.2 and (4.1) lead to

$$\frac{1}{2\mu_2}\|\sigma - \sigma_{CR}\|^2 + E_{NC}(u_{CR}) \leq E(u) + \kappa\|h_{\mathcal{T}} f\|\ \|(1 - \Pi_0)\nabla u\|. \tag{4.9}$$

The estimate (4.4) and the Cauchy–Schwarz inequality imply

$$\begin{aligned}\frac{1}{2\mu_2}\|\sigma - \sigma_{CR}\|^2 + |E(u) - E_{NC}(u_{CR})| \\ \leq \max\left\{F(u_{CR} - u_3) + \|\sigma - \Pi_0\sigma\|\ |||u_{CR} - u_3|||_{NC}, \kappa\|h_{\mathcal{T}} f\|\ |||u|||\right\}.\end{aligned}$$

The Young inequality shows

$$\|\sigma - \Pi_0\sigma\|\ |||u_{CR} - u_3|||_{NC} \leq \frac{1}{4\mu_2}\|\sigma - \Pi_0\sigma\|^2 + \mu_2|||u_{CR} - u_3|||_{NC}^2.$$

The combination with (4.7) concludes the proof. ∎

5. Error analysis of RT-MFEM.

5.1. A priori error analysis. The subsequent result generalizes Theorem 5.2 in [13] for $\varepsilon \to 0$. Notice that the Fortin interpolation operator I_F maps $Q(f) \cap H^s(\Omega;\mathbb{R}^2)$ onto $Q(f,\mathcal{T})$ for any $s > 0$. Hence $E^*(\sigma_{RT}) - E^*(I_F\sigma) \geq 0$ holds on the LHS of the subsequent error estimate.

Theorem 5.1 (a priori error estimate). *Given any $\xi \in L^2(\Omega;\mathbb{R}^2)$ with $\xi(x) \in \partial W^*(I_F\sigma)$ for a.e. $x \in \Omega$, the discrete stress σ_{RT} and the constant $C_2 := 2C_F\|f\|/(\mu_1 j_{1,1})$ satisfy*

$$\frac{1}{2\mu_2}\|\sigma - \sigma_{RT}\|^2 + E^*(\sigma_{RT}) - E^*(I_F\sigma) \leq \|\xi\|\ \|\sigma - I_F\sigma\| + C_2 \mathrm{osc}(f,\mathcal{T})$$

with the first positive root $j_{1,1} = 3.8317059702$ of the Bessel function of the first kind [22].

Proof. Recall that $\sigma \in H^{1/2-\epsilon}(\Omega;\mathbb{R}^2)$ for any $0 < \epsilon < 1/2$ [21] and let

$$I_F : H^{1/2-\epsilon}(\Omega;\mathbb{R}^2) \to RT_0(\mathcal{T})$$

be the Fortin interpolation operator [7] with respect to $\mathcal{T}$ with

$$\int_E (\sigma - I_F\sigma)\cdot \nu_E ds = 0 \qquad \text{for all } E \in \mathcal{E}.$$

The choice $\alpha := \sigma_{RT}$, $\beta := \sigma$, and $b := \nabla u$ in Lemma 3.4 leads to

$$\frac{1}{2\mu_2}\|\sigma - \sigma_{RT}\|^2 \leq E^*(\sigma) - E^*(\sigma_{RT}) - \int_\Omega \nabla u \cdot (\sigma_{RT} - \sigma) dx. \tag{5.1}$$

An integration by parts shows

$$\begin{aligned} -\int_\Omega \nabla u \cdot (\sigma_{RT} - \sigma) dx &= \int_\Omega u \,\mathrm{div}(\sigma_{RT} - \sigma) dx \\ &= \int_\Omega (u - \Pi_0 u)\ (f - \Pi_0 f) dx. \end{aligned}$$

A piecewise Poincaré inequality applies in the last step with the constant $h_T/j_{1,1}$ from [22]. Hence the last term is bounded by $|||u|||/j_{1,1}\ \mathrm{osc}(f,\mathcal{T})$. This and $\sigma_{RT} = \arg\max E^*(Q(f,\mathcal{T}))$ imply

$$\begin{aligned} &\frac{1}{2\mu_2}\|\sigma - \sigma_{RT}\|^2 + E^*(\sigma_{RT}) - E^*(I_F\sigma) \\ &\quad \leq E^*(\sigma) - E^*(I_F\sigma) + |||u|||/j_{1,1}\ \mathrm{osc}(f,\mathcal{T}). \end{aligned}$$

The choice $\alpha := \sigma$, $\beta := I_F\sigma$, and $b := \xi(x) \in \partial W^*(I_F\sigma)$ in Lemma 3.4 leads to

$$\frac{1}{2\mu_2}|\sigma - I_F\sigma|^2 + \xi\cdot(\sigma - I_F\sigma) \leq W^*(\sigma) - W^*(I_F\sigma) \qquad \text{a.e. in } \Omega.$$

Hence,

$$\frac{1}{2\mu_2}\|\sigma - I_F\sigma\|^2 + E^*(\sigma) - E^*(I_F\sigma) \leq \int_\Omega \xi \cdot (I_F\sigma - \sigma) dx.$$

The Cauchy–Schwarz inequality and (4.7) conclude the proof. ∎

5.2. A posteriori error analysis. The stress error control in the subsequent error estimate may formally follow from Theorem 5.3 in [13] as $\varepsilon \to 0$, while the energy error control is new.

THEOREM 5.2 (a posteriori error estimate). *For any $\xi \in L^2(\Omega;\mathbb{R}^2)$ with $\xi(x) \in \partial W^*(\sigma_{RT})$ for a.e. $x \in \Omega$, the discrete stress σ_{RT} satisfies*

$$\frac{1}{4\mu_2}\|\sigma - \sigma_{RT}\|^2 + |E^*(\sigma) - E^*(\sigma_{RT})| \\ \leq \max\left\{\min_{v\in V}\left(\mu_2\|\nabla v - \xi\|^2 + |||v|||\ \mathrm{osc}(f,\mathcal{T})/j_{1,1}\right), |||u|||\ \mathrm{osc}(f,\mathcal{T})/j_{1,1}\right\}.$$

Proof. The choice $\alpha := \sigma$, $\beta := \sigma_{RT}$, and $b := \xi$ in Lemma 3.4 leads to

$$\frac{1}{2\mu_2}\|\sigma - \sigma_{RT}\|^2 + E^*(\sigma) - E^*(\sigma_{RT}) \leq -\int_\Omega \xi\cdot(\sigma - \sigma_{RT})dx. \tag{5.2}$$

For all $v \in V$, the upper bound equals

$$\int_\Omega (\nabla v - \xi)\cdot(\sigma - \sigma_{RT})dx - \int_\Omega \nabla v\cdot(\sigma - \sigma_{RT})dx \\ \leq \min_{v\in V}\left(\|\nabla v - \xi\|\ \|\sigma - \sigma_{RT}\| + |||v|||\ \mathrm{osc}(f,\mathcal{T})/j_{1,1}\right).$$

The choice $\alpha := \sigma_{RT}$, $\beta := \sigma$, and $b := \nabla u$ in Lemma 3.4 leads to

$$\frac{1}{2\mu_2}\|\sigma - \sigma_{RT}\|^2 + E^*(\sigma_{RT}) - E^*(\sigma) \leq |||u|||\ \mathrm{osc}(f,\mathcal{T})/j_{1,1}. \tag{5.3}$$

The combination of (5.2)–(5.3) leads to

$$\frac{1}{2\mu_2}\|\sigma - \sigma_{RT}\|^2 + |E^*(\sigma) - E^*(\sigma_{RT})| \\ \leq \max\left\{\min_{v\in V}\left(\|\nabla v - \xi\|\ \|\sigma - \sigma_{RT}\| + |||v|||\ \mathrm{osc}(f,\mathcal{T})/j_{1,1}\right),\right. \\ \left. |||u|||\ \mathrm{osc}(f,\mathcal{T})/j_{1,1}\right\}. \tag{5.4}$$

The Young inequality shows that

$$\|\nabla v - \xi\|\ \|\sigma - \sigma_{RT}\| \leq \mu_2\|\nabla v - \xi\|^2 + \frac{1}{4\mu_2}\|\sigma - \sigma_{RT}\|^2.$$

The combination of above estimates concludes the proof. ∎

6. Error analysis of dRT-MFEM. This section analyzes the error of the dRT-MFEM.

6.1. A priori error analysis. Theorems 3.1 and 4.1 allow an immediate a priori error estimate.

THEOREM 6.1 (a priori error estimate). *The discrete stress σ_{dRT} satisfies*

$$\|\sigma - \sigma_{dRT}\|^2 + |E^*(\sigma) - E^*_d(\sigma_{dRT})| \\ \lesssim \|h_\mathcal{T}(\Pi_0 f)\|^2 \\ + \max\left\{\|h_\mathcal{T} f\|\ |||u - I_{NC}u|||, \left(\mathrm{osc}(f,\mathcal{T}) + \|\sigma - \Pi_0\sigma\|\right)|||u - u_{CR}|||_{NC}\right\}.$$

Proof. The triangle inequality and Theorem 3.1 lead to

$$\frac{1}{2}\|\sigma - \sigma_{dRT}\|^2 \le \|\sigma - \Pi_0\sigma_{dRT}\|^2 + \|\Pi_0\sigma_{dRT} - \sigma_{dRT}\|^2$$
$$\le \|\sigma - \sigma_{CR}\|^2 + \|h_{\mathcal{T}}(\Pi_0 f)\|^2.$$

The equalities $E^*(\sigma) = E(u)$ and $E_d^*(\sigma_{dRT}) = E_{NC}(u_{CR})$ (from Theorem 3.1) imply

$$\begin{aligned}&\frac{1}{4\mu_2}\|\sigma - \sigma_{dRT}\|^2 + |E^*(\sigma) - E_d^*(\sigma_{dRT})|\\ &\quad\le \frac{1}{2\mu_2}\|\sigma - \sigma_{CR}\|^2 + |E(u) - E_{NC}(u_{CR})| + \frac{1}{2\mu_2}\|h_{\mathcal{T}}(\Pi_0 f)\|^2.\end{aligned} \tag{6.1}$$

This and Theorem 4.1 conclude the proof. ∎

6.2. Subgradients of the discrete dual problem. The further a posteriori error analysis requires that the arising subgradients are the piecewise gradients of minimizers of E_{NC} in $CR_0^1(\mathcal{T})$.

LEMMA 6.2 ($\Pi_0(-\partial E_d^*(\sigma_{dRT})) = \nabla_{NC} u_{CR}$). *The piecewise integral mean $\Pi_0\xi$ of any subgradient ξ of the function $\int_\Omega W^*(\Pi_0\sigma_{dRT})dx$ with $-\xi \in \partial\chi_{Q(f,\mathcal{T})}\ (\sigma_{dRT})$ equals the piecewise gradient of some minimizer u_{CR} in $(CR_0^1(\mathcal{T}))$,*

$$\Pi_0\xi = \nabla_{NC} u_{CR} \in \partial W^*(\sigma_{CR}).$$

Proof. Let $\chi_{Q(f,\mathcal{T})}$ denote the indicator function [20] of the convex closed subset $Q(f,\mathcal{T}) \subseteq RT_0(\mathcal{T})$ with $\chi_{Q(f,\mathcal{T})}(\tau_h) := 0$ for $\tau_h \in Q(f,\mathcal{T})$ and $\chi_{Q(f,\mathcal{T})}(\tau_h) := +\infty$ otherwise.

Define the function $\Phi(\tau) := \int_\Omega W^*(\Pi_0\tau)dx$ for any $\tau \in L^2(\Omega;\mathbb{R}^2)$. The minimizer σ_{dRT} of $\Phi + \chi_{Q(f,\mathcal{T})}$ satisfies

$$0 \in \partial\Phi(\sigma_{dRT}) + \partial\chi_{Q(f,\mathcal{T})}(\sigma_{dRT}).$$

The sum rule for the subgradient [20, Theorem 2.32] is already utilized in the preceding formula and shows that there exists $\xi \in \partial\Phi(\sigma_{dRT}) \subset L^2(\Omega;\mathbb{R}^2)$ with $-\xi \in \partial\chi_{Q(f,\mathcal{T})}(\sigma_{dRT})$. The latter inclusion reads

$$-\int_\Omega \xi\cdot(\tau_{RT} - \sigma_{dRT})dx \le 0 \quad \text{ for all } \tau_{RT} \in Q(f,\mathcal{T}).$$

Since $\sigma_{dRT} \in Q(f,\mathcal{T})$, any $\tau_{RT} \in \sigma_{dRT} + Q(0,\mathcal{T})$ belongs to $Q(f,\mathcal{T})$. Hence

$$\xi \in Q(0,\mathcal{T})^\perp := \text{orthogonal complement of } Q(0,\mathcal{T}) \text{ in } L^2(\Omega;\mathbb{R}^2).$$

Notice that $Q(0,\mathcal{T}) \subset \mathcal{P}_0(\mathcal{T},\mathbb{R}^2)$ and so $\Pi_0\xi \in Q(0,\mathcal{T})^\perp$. The discrete Helmholtz decomposition [3] shows for a simply connected domain Ω that there exists some $u_h \in CR_0^1(\mathcal{T})$ with $\Pi_0\xi = \nabla_{NC} u_h$. (The curl contribution vanishes because of $\Pi_0\xi \in Q(0,\mathcal{T})^\perp$.)

On the other hand, for all $\tau \in L^2(\Omega;\mathbb{R}^2)$,

$$\int_\Omega \xi\cdot(\tau - \sigma_{dRT})dx \le \Phi(\tau) - \Phi(\sigma_{dRT}) = \int_\Omega W^*(\Pi_0\tau)dx - \int_\Omega W^*(\Pi_0\sigma_{dRT})dx.$$

Given any $T \in \mathcal{T}$ and $A \in \mathbb{R}^2$, set

$$\tau := \begin{cases} \sigma_{dRT} + A & \text{in } T,\\ \sigma_{dRT} & \text{in } \Omega\setminus T.\end{cases}$$

This and $\Pi_0\xi = \nabla_{NC} u_h$ imply, for any $T \in \mathcal{T}$ and $A \in \mathbb{R}^2$, that

$$\nabla_{NC} u_h \cdot A = \left(\fint_T \xi dx \right) \cdot A \leq W^*(\Pi_0\sigma_{dRT} + A) - W^*(\Pi_0\sigma_{dRT}).$$

In other words, $\nabla_{NC} u_h \in \partial W^*(\Pi_0\sigma_{dRT})$. This and $\Pi_0\sigma_{dRT} = \sigma_{CR}$ from Theorem 3.1 plus the duality relation imply $\sigma_{CR} = DW(\nabla_{NC} u_h)$.

It remains to prove that u_h minimizes E_{NC} in $CR_0^1(\mathcal{T})$. Let u_{CR} be some minimizer of E_{NC} in $CR_0^1(\mathcal{T})$ such that $\sigma_{CR} = DW(\nabla_{NC} u_{CR}) = DW(\nabla_{NC} u_h)$. The choice $a := \nabla_{NC} u_h$ and $b := \nabla_{NC} u_{CR}$ in Lemma 3.4 shows

$$\begin{aligned} 0 &\leq \int_\Omega W(\nabla_{NC} u_{CR}) dx - \int_\Omega W(\nabla_{NC} u_h) dx - \int_\Omega \sigma_{CR} \cdot \nabla_{NC}(u_{CR} - u_h) dx \\ &= E_{NC}(u_{CR}) - E_{NC}(u_h). \end{aligned}$$

Since $u_{CR} \in \arg\min E_{NC}(CR_0^1(\mathcal{T}))$, the upper bound is nonpositive. Hence, $E_{NC}(u_{CR}) = E_{NC}(u_h)$; that is, u_h minimizes E_{NC} in $CR_0^1(\mathcal{T})$. ∎

6.3. A posteriori error analysis. This subsection is devoted to an a posteriori error analysis of the dRT-MFEM.

THEOREM 6.3 (first a posteriori error estimate). *The discrete stress σ_{dRT} and the constant $C_1 := 2\kappa C_F \|f\|/\mu_1$ satisfy*

$$\begin{aligned} &\frac{1}{8\mu_2}\|\sigma - \sigma_{dRT}\|^2 + |E^*(\sigma) - E_d^*(\sigma_{dRT})| \\ &\quad \leq \frac{1}{2\mu_2}\|h_\mathcal{T} f\|^2 \\ &\qquad + \max\left\{ \frac{\||u_3\||}{j_{1,1}} \operatorname{osc}(f, \mathcal{T}) + 2\mu_2 \||u_3 - I_{NC} u_3\||^2, C_1\|h_\mathcal{T} f\| \right\}. \end{aligned} \tag{6.2}$$

Proof. The choice $\alpha := \sigma$, $\beta := \Pi_0\sigma_{dRT} = \sigma_{CR}$, and $b := \nabla_{NC} u_{CR}$ in Lemma 3.4 leads to

$$\frac{1}{2\mu_2}\|\sigma - \Pi_0\sigma_{dRT}\|^2 + E^*(\sigma) - E_d^*(\sigma_{dRT}) \leq -\int_\Omega \nabla_{NC} u_{CR} \cdot (\sigma - \Pi_0\sigma_{dRT}) dx.$$

The conforming $\mathcal{P}_3$ companion $u_3 \in \mathcal{P}_3(\mathcal{T}) \cap V$ with $u_{CR} = I_{NC} u_3$ from Lemma 3.3 shows

$$\begin{aligned} &-\int_\Omega (\sigma - \Pi_0\sigma_{dRT}) \cdot \nabla_{NC} u_{CR} dx \\ &\quad = -\int_\Omega (\sigma - \sigma_{dRT}) \cdot \nabla_{NC}(I_{NC} u_3 - u_3) dx - \int_\Omega (\sigma - \sigma_{dRT}) \cdot \nabla u_3 dx \\ &\quad = \int_\Omega (\sigma - \sigma_{dRT}) \cdot (1 - \Pi_0)\nabla u_3 dx + \int_\Omega u_3 \operatorname{div}(\sigma - \sigma_{dRT}) dx. \end{aligned}$$

The combination of the preceding results reads

$$\begin{aligned} &\frac{1}{2\mu_2}\|\sigma - \sigma_{CR}\|^2 + E^*(\sigma) - E_d^*(\sigma_{dRT}) \\ &\quad \leq \int_\Omega (\sigma - \sigma_{dRT}) \cdot (1 - \Pi_0)\nabla u_3 dx - \int_\Omega (u_3 - \Pi_0 u_3)\ (1 - \Pi_0) f dx. \end{aligned} \tag{6.3}$$

The sum of (6.3) and (4.1) plus Theorem 3.1 show that

$$\frac{1}{2\mu_2}\|\sigma-\sigma_{CR}\|^2+|E^*(\sigma)-E_d^*(\sigma_{dRT})| \le \max\Big\{F(u-I_{NC}u), \int_\Omega(\sigma-\sigma_{dRT})\cdot(1-\Pi_0)\nabla u_3 dx - \int_\Omega(u_3-\Pi_0 u_3)\ (1-\Pi_0)f dx\Big\}.$$

The inequality (6.1) implies

$$\frac{1}{4\mu_2}\|\sigma-\sigma_{dRT}\|^2+|E^*(\sigma)-E_d^*(\sigma_{dRT})| \le \frac{1}{2\mu_2}\|h_{\mathcal{T}}f\|^2+\max\Big\{F(u-I_{NC}u), \int_\Omega(\sigma-\sigma_{dRT})\cdot(1-\Pi_0)\nabla u_3 dx - \int_\Omega(u_3-\Pi_0 u_3)\ (1-\Pi_0)f dx\Big\}.$$

The Cauchy–Schwarz inequality shows that

$$-\int_\Omega(u_3-\Pi_0u_3)\ (f-\Pi_0 f)dx \le \frac{|||u_3|||}{j_{1,1}}\operatorname{osc}(f,\mathcal{T}),$$
$$\int_\Omega(\sigma-\sigma_{dRT})\cdot(1-\Pi_0)\nabla u_3 dx \le \|\sigma-\sigma_{dRT}\|\ |||I_{NC}u_3-u_3|||_{NC}.$$

The Young inequality shows

$$\|\sigma-\sigma_{dRT}\|\ |||I_{NC}u_3-u_3|||_{NC} \le \frac{1}{8\mu_2}\|\sigma-\sigma_{dRT}\|^2+2\mu_2|||I_{NC}u_3-u_3|||_{NC}^2.$$

The combination of the preceding displayed inequalities concludes the proof. ∎

THEOREM 6.4 (second a posteriori error estimate). *The discrete stress σ_{dRT} satisfies*

(6.4)
$$\frac{1}{4\mu_2}\|\sigma-\sigma_{dRT}\|^2+\frac{1}{2\mu_2}\|\sigma-\sigma_{CR}\|^2 \le E_d^*(\sigma_{dRT})-E^*(\sigma_{dRT})+\frac{2C_F\|f\|/\mu_1+|||u_3|||}{j_{1,1}}\operatorname{osc}(f,\mathcal{T})+\mu_2|||I_{NC}u_3-u_3|||^2.$$

Proof. The choice $\alpha:=\sigma_{dRT}$, $\beta:=\sigma$, and $b:=\nabla u$ in Lemma 3.4 leads to

$$\frac{1}{2\mu_2}\|\sigma-\sigma_{dRT}\|^2 \le E^*(\sigma)-E^*(\sigma_{dRT})-\int_\Omega \nabla u\cdot(\sigma_{dRT}-\sigma)dx = E^*(\sigma)-E^*(\sigma_{dRT})+\int_\Omega u\ (1-\Pi_0)f dx. \tag{6.5}$$

The sum of (6.3) and (6.5) implies

$$\frac{1}{2\mu_2}(\|\sigma-\sigma_{dRT}\|^2+\|\sigma-\sigma_{CR}\|^2) \le E_d^*(\sigma_{dRT})-E^*(\sigma_{dRT})+\int_\Omega(f-\Pi_0 f)\ (u-u_3)dx + \int_\Omega(\sigma-\sigma_{dRT})\cdot(1-\Pi_0)\nabla u_3 dx.$$

The Cauchy–Schwarz inequality, the triangle inequality, plus (4.7) show that

$$\int_\Omega (f-\Pi_0 f)\ (u-u_3)dx \le \frac{|||u-u_3|||}{j_{1,1}}\mathrm{osc}(f,\mathcal{T}) \le \frac{2C_F\|f\|/\mu_1 + |||u_3|||}{j_{1,1}}\mathrm{osc}(f,\mathcal{T}).$$

The Young inequality and $\Pi_0\nabla u_3 = \nabla_{NC} I_{NC} u_3$ show that

$$\int_\Omega (\sigma-\sigma_{dRT})\cdot(1-\Pi_0)\nabla u_3 dx \le \frac{1}{4\mu_2}\|\sigma-\sigma_{dRT}\|^2 + \mu_2 |||I_{NC}u_3 - u_3|||_{NC}^2.$$

The combination of the three preceding displayed estimates concludes the proof. ∎

THEOREM 6.5 (third a posteriori error estimate). *For any $\xi \in L^2(\Omega;\mathbb{R}^2)$ with $\xi(x)\in\partial W^*(\sigma_{dRT})$ for a.e. $x\in\Omega$, the constant $C_1 := 2\kappa C_F\|f\|/\mu_1$ and the discrete stress σ_{dRT} satisfy*

$$\frac{1}{2\mu_2}\|\sigma-\sigma_{dRT}\|^2 + |E^*(\sigma)-E^*_d(\sigma_{dRT})| \le \max\left\{\min_{v\in V}\Big(\mu_2\|\nabla v-\xi\|^2 + |||v|||\ \mathrm{osc}(f,\mathcal{T})/j_{1,1}\Big), C_1\|h_\mathcal{T} f\|\right\}.$$

The proof of Theorem 6.5 utilizes the following Lemma 6.6.

LEMMA 6.6. *It holds that $\frac{1}{2\mu_2}\|\sigma_{dRT}-\Pi_0\sigma_{dRT}\|^2 + E^*(\sigma_{dRT}) \le E^*_d(\sigma_{dRT})$.*

Proof. The choice $\alpha := \sigma_{dRT}$, $\beta := \Pi_0\sigma_{dRT}$, and $b := \nabla_{NC}u_{CR}$ in Lemma 3.4 leads to

$$\frac{1}{2\mu_2}\|\sigma_{dRT}-\Pi_0\sigma_{dRT}\|^2 \le E^*_d(\sigma_{dRT}) - E^*(\sigma_{dRT}) + \int_\Omega \nabla_{NC}u_{CR}\cdot(\sigma_{dRT}-\sigma_{CR})dx.$$

Lemma 3.5 and $\sigma_{dRT}\in Q(f,\mathcal{T})$ show that the integral vanishes. This concludes the proof. ∎

Proof of Theorem 6.5. The choice $\alpha := \sigma$, $\beta := \sigma_{dRT}$, and $b := \xi$ in Lemma 3.4 leads to

$$\frac{1}{2\mu_2}\|\sigma-\sigma_{dRT}\|^2 + E^*(\sigma) - E^*(\sigma_{dRT}) \le -\int_\Omega \xi\cdot(\sigma-\sigma_{dRT})dx.$$

For all $v\in V$, the upper bound of this estimate equals

$$\int_\Omega (\nabla v-\xi)\cdot(\sigma-\sigma_{dRT})dx - \int_\Omega \nabla v\cdot(\sigma-\sigma_{dRT})dx \le \min_{v\in V}\Big(\|\nabla v-\xi\|\ \|\sigma-\sigma_{dRT}\| + |||v|||\ \mathrm{osc}(f,\mathcal{T})/j_{1,1}\Big).$$

Lemma 6.6 implies

$$\frac{1}{2\mu_2}\|\sigma-\sigma_{dRT}\|^2 + \frac{1}{2\mu_2}\|\sigma_{dRT}-\Pi_0\sigma_{dRT}\|^2 + E^*(\sigma) - E^*_d(\sigma_{dRT}) \le \min_{v\in V}\Big(\|\nabla v-\xi\|\ \|\sigma-\sigma_{dRT}\| + |||v|||\ \mathrm{osc}(f,\mathcal{T})/j_{1,1}\Big). \tag{6.6}$$

The sum of (6.6) and (4.1) plus Theorem 3.1 show that

$$\frac{3}{4\mu_2}\|\sigma-\sigma_{dRT}\|^2 + |E^*(\sigma)-E^*_d(\sigma_{dRT})| \le \max\left\{\min_{v\in V}\Big(\|\nabla v-\xi\|\ \|\sigma-\sigma_{dRT}\| + |||v|||\ \mathrm{osc}(f,\mathcal{T})/j_{1,1}\Big), F(u-I_{NC}u)\right\}.$$

The Young inequality leads to

$$\|\nabla v - \xi\| \; \|\sigma - \sigma_{dRT}\| \le \mu_2 \|\nabla v - \xi\|^2 + \frac{1}{4\mu_2}\|\sigma - \sigma_{dRT}\|^2.$$

The combination of the preceding four displayed inequalities concludes the proof. ∎

7. Numerical experiments. This section is devoted to the numerical investigation of the lowest-order schemes of CFEM, NCFEM, MFEM for the optimal design problem on three different domains.

7.1. Numerical realization. The edge-oriented basis functions ψ_E for any interior edge $E \in \mathcal{E}(\Omega)$ in the triangulation $\mathcal{T}$ and their enumeration $\psi_1, \ldots, \psi_m$ at hand allows for the representation $u_{CR} = \sum_{j=1}^m x_j \psi_j$ with the unknown coefficient vector $x = (x_1, \ldots, x_m)$. The data structures and the discrete Euler–Lagrange equations are realized as in [9] and then minimized with the MATLAB standard function `fminunc` and default parameters and the input of E_{NC}, DE_{NC}, and D^2E_{NC} at x. Throughout this section, $\mu_1 = 1, \mu_2 = 2$, $t_1 = \sqrt{2\lambda\mu_1/\mu_2}$, $t_2 = \sqrt{2\lambda\mu_2/\mu_1}$ for different values of λ and $C_1 = 0.3166\, \|f\|$.

7.2. A posteriori error control. The numerical experiments concern the practical application of the a posteriori error estimates (2.2), (4.5), (6.2), (6.4) and their efficiency. Denote the left-hand side (LHS) of the four estimates by $LHS(2.2)$, $LHS(4.5)$, $LHS(6.2)$, and $LHS(6.4)$. The guaranteed upper bounds (GUB) read

$$\begin{aligned}
GUB(2.2) &= \sqrt{\sum_{E\in\mathcal{E}(\Omega)} \eta_E{}^2} + \operatorname{osc}(f, \mathcal{T});\\
GUB(4.5) &= \max\left\{F(u_{CR} - u_3) + \mu_2 |||u_3 - I_{NC}u_3|||^2_{NC}, C_1\|h_\mathcal{T} f\|\right\};\\
GUB(6.2) &= \max\left\{\frac{|||u_3|||}{j_{1,1}}\operatorname{osc}(f,\mathcal{T}) + 2\mu_2|||u_3 - I_{NC}u_3|||^2, C_1\|h_\mathcal{T} f\|\right\}\\
&\quad + \frac{1}{2\mu_2}\|h_\mathcal{T} f\|^2;\\
GUB(6.4) &= E_d^*(\sigma_{dRT}) - E^*(\sigma_{dRT}) + \frac{2C_F\|f\|/\mu_1 + |||u_3|||}{j_{1,1}}\operatorname{osc}(f,\mathcal{T})\\
&\quad + \mu_2|||u_3 - I_{NC}u_3|||^2.
\end{aligned}$$

The triangulations are either uniform with successive red-refinement or with an adaptive mesh-refinement algorithm with initial mesh $\mathcal{T}_0$, and then, for any triangle T of a triangulation $\mathcal{T}_\ell$ at level $\ell = 0, 1, 2, 3 \ldots$, set

$$\eta^2(T) = |||u_3 - I_{NC}u_3|||^2_{L^2(T)} + \|h_\mathcal{T} f\|^2_{L^2(T)}.$$

Given all those contributions, mark some set $\mathcal{M}_\ell$ of triangles in $\mathcal{T}_\ell$ of minimal cardinality with the bulk criterion

$$1/2 \sum_{T\in\mathcal{T}_\ell} \eta_\ell^2(T) \le \sum_{T\in\mathcal{M}_\ell} \eta_\ell^2(T).$$

The refinement of all triangles in $\mathcal{M}_\ell$ plus minimal further refinements to avoid hanging nodes lead to the triangulation $\mathcal{T}_{\ell+1}$ within the newest-vertex bisection. The choice of the refinement-indicator $\eta(T)$ is motivated by the convergence theory of adaptive mesh-refining algorithms, e.g., in the review article [11] with further details on the mesh-refinement. The convergence history plots display the $LHS(2.2)$, $LHS(4.5)$, $LHS(6.2)$, $LHS(6.4)$ and the upper bounds $GUB(2.2)$, $GUB(4.5)$, $GUB(6.2)$, $GUB(6.4)$ as a function of the number of degrees of freedom (ndof) in a log-log scale.

7.3. Manufactured example. Consider the optimal design problem on the square domain $\Omega := (-1,1)^2$ with the exact solution $u(x_1,x_2) = (1-x_1^2)(1-x_2^2)$ and right-hand side $f = -\mathrm{div}DW(\nabla u)$ for $\lambda = 0.0084$ as in [4]. The reference value for the minimal energy $E = -2.82789$ stems from Aitken extrapolation. Figure 1 displays four GUB and the corresponding error terms (LHS) of the four estimates from (2.2), (4.5), (6.2), and (6.4) as explained in subsection 7.2 for uniform mesh-refinements. Figure 2 presents the computed values for uniform and adaptive mesh-refinement. The

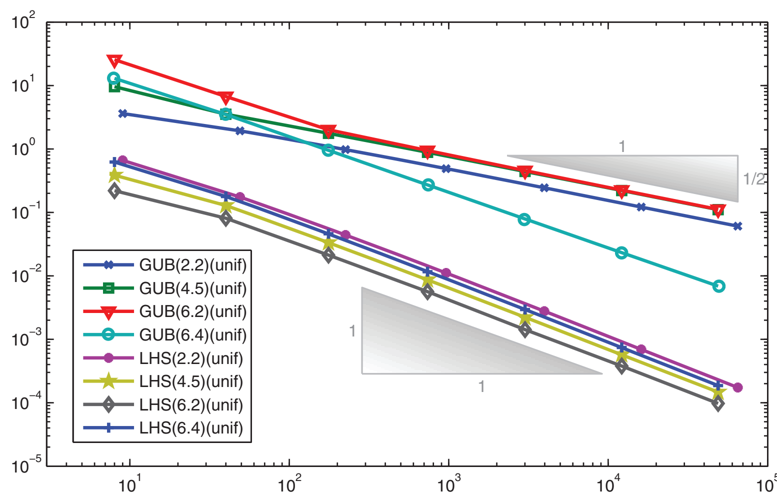

FIG. 1. *Convergence history on square domain for uniform mesh-refinements.*

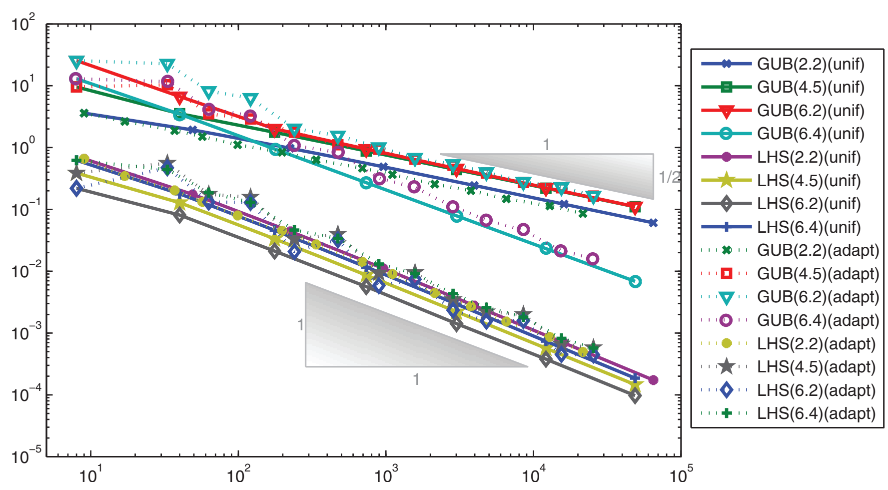

FIG. 2. *Convergence history of three methods on square domain.*

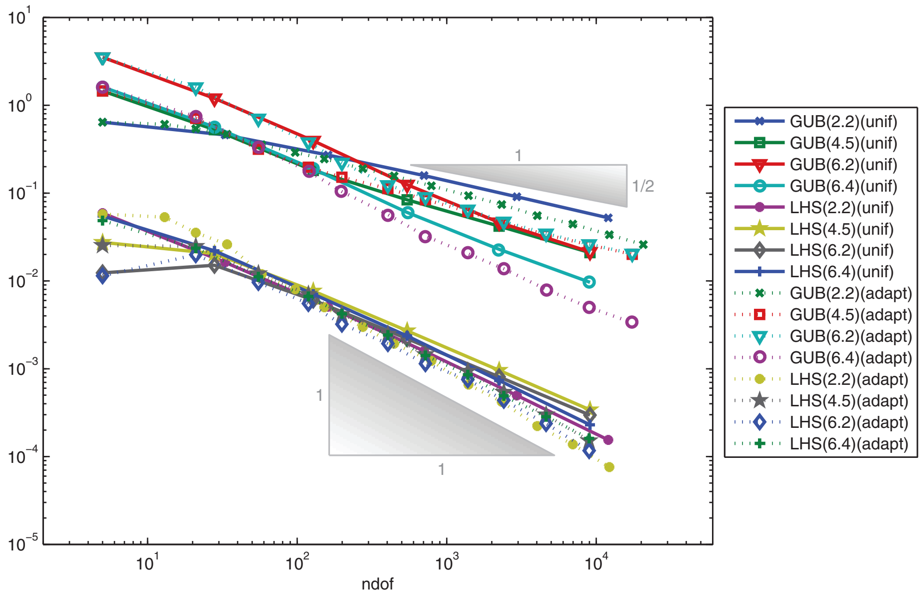

FIG. 3. *Convergence history of three methods on L-shaped domain.*

exact solution is smooth and hence uniform mesh-refining leads to optimal convergence rates (on structured grids with possible super convergence phenomena) and hence the adaptive mesh-refining is not necessarily better (on unstructured grids without higher symmetry). Lemma 3.3 and (4.8) imply that $|||u_3|||$ is computable and $(2C_F\|f\|/\mu_1 + |||u_3|||)/j_{1,1}$ is bounded by some generic constant.

7.4. L-shaped domain. Consider the optimal design problem on the L-shaped domain $\Omega := [-1,1]^2\backslash(0,1] \times (0,-1]$ with $f \equiv 1$ for $\lambda = 0.0143$ as in [4]. The extrapolated energy reads $E = -0.0963$. Figure 3 displays the convergence history of the three methods for uniform and adaptive mesh-refinement. Since the constant right-hand side $f \equiv 1$ leads to vanishing oscillations $\mathrm{osc}(f,\mathcal{T}) = 0$, the global upper bound in (6.4) is fully computable.

7.5. Slit domain. Consider the optimal design problem on the slit domain with $f \equiv 1$ for $\lambda = 0.0163$. The extrapolated energy reads $E = -0.1464$. Figure 4 displays the convergence history of the three methods for uniform and adaptive mesh-refinement. The constant right-hand side $f \equiv 1$ leads to a fully computable upper bound (6.4) as in the previous example.

7.6. Conclusions. The proposed the dRT-MFEM of the optimal design problem is equivalent to CR-NCFEM. The convergence analysis of dRT-MFEM combines a priori convergence of CFEM with the efficient a posteriori error control of MFEM. The numerical examples show that the convergence results of $\mathcal{P}_1$-CFEM, CR-NCFEM, and dRT-MFEM are consistent with the theoretical analysis: the empirical convergence rates for the three methods are comparable. The a posteriori error analysis suffers from the reliability-efficiency gap except for $GUB(6.4)$: Theorem 6.4 behaves efficiently in the sense that it captures the convergence rate of $LHS(6.4)$ and thereby overcomes the reliability-efficiency gap [14] of conforming discretizations.

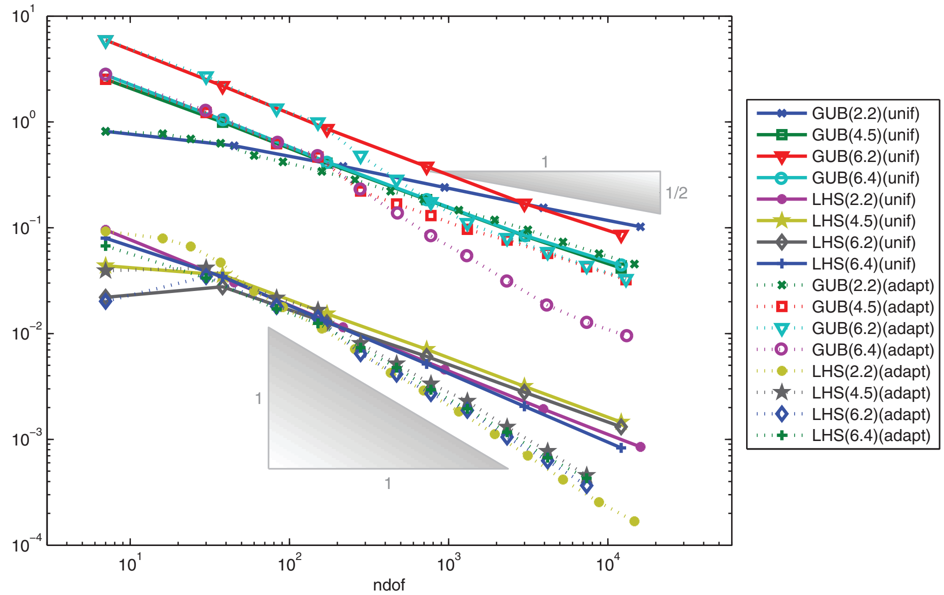

FIG. 4. *Convergence history of three methods on slit domain.*

REFERENCES

[1] T. ARBOGAST AND Z. X. CHEN, *On the implementation of mixed methods as nonconforming methods for second-order elliptic problems*, Math. Comp., 64 (1995), pp. 943–972.

[2] D. N. ARNOLD AND F. BREZZI, *Mixed and nonconforming finite element methods: Implementation, postprocessing and error estimates*, ESAIM Math. Model. Numer. Anal., 19 (1985), pp. 7–32.

[3] D. N. ARNOLD AND R. S. FALK, *Analysis of a linear-linear finite element for the Reissner-Mindlin plate model*, Math. Models Methods Appl. Sci., 7 (1997), pp. 217–238.

[4] S. BARTELS AND C. CARSTENSEN, *A convergent adaptive finite element method for an optimal design problem*, Numer. Math., 108 (2008), pp. 359–385.

[5] S. C. BRENNER, *Two-level additive Schwarz preconditioners for nonconforming finite element methods*, Math. Comp., 65 (1996), pp. 897–921.

[6] S. C. BRENNER AND L. SCOTT, *The Mathematical Theory of Finite Element Methods*, 3rd ed., Texts in Appl. Math. 15, Springer, New York, 2008.

[7] F. BREZZI AND M. FORTIN, *Mixed and Hybrid Finite Element Methods*, Springer, New York, 1991.

[8] C. CARSTENSEN, *Convergence of an adaptive FEM for a class of degenerate convex minimization problems*, IMA J. Numer. Anal., 28 (2008), pp. 423–439.

[9] C. CARSTENSEN AND C. BAHRIAWATI, *Three MATLAB implementations of the lowest-order Raviart-Thomas MFEM with a posteriori error control*, Comput. Methods Appl. Math., 5 (2005), pp. 333–361.

[10] C. CARSTENSEN AND D. GALLISTL, *Guaranteed lower eigenvalue bounds for the biharmonic equation*, Numer. Math.,126 (2014), pp. 33–51.

[11] C. CARSTENSEN, M. FEISCHL, M. PAGE, AND D. PRAETORIUS, *Axioms of adaptivity*, Comput. Methods Appl. Math., 67 (2014), pp. 1195–1253.

[12] C. CARSTENSEN, J. GEDICKE, AND D. RIM, *Explicit error estimates for Courant, Crouzeix-Raviart and Raviart-Thomas finite element methods*, J. Comput. Math., 30 (2012), pp. 337–353.

[13] C. CARSTENSEN, D. GÜNTHER, AND H. RABUS, *Mixed finite element method for a degenerate convex variational problems from topology optimization*, SIAM J. Numer. Anal., 50 (2012), pp. 522–543.

[14] C. CARSTENSEN AND K. JOCHIMSEN, *Adaptive finite element methods for microstructures? Numerical experiments for a 2-well benchmark*, Computing, 71 (2003), pp. 175–204.

[15] C. Carstensen and S. Müller, *Local stress regularity in scalar nonconvex variational problems*, SIAM J. Math. Anal., 34 (2002), pp. 495–509.
[16] C. Carstensen and P. Plecháč, *Numerical solution of the scalar double-well problem allowing microstructure*, Math. Comp., 66 (1997), pp. 997–1026.
[17] A. Cherkave, *Variational Methods for Structural Optimization*, Springer, New York, 2000.
[18] D. A. French, *On the convergence of finite-element approximation of a relaxed varitional problem*, SIAM J. Numer. Anal., 27 (1990), pp. 419–436.
[19] J. Goodman, R. Kohn, and L. Reyna, *Numerical study of a relaxed varitional problem from optimal design*, Comput. Methods Appl. Mech. Engrg., 57 (1986), pp. 107–127.
[20] W. Han, *A Posteriori Error Analysis via Duality Theory: With Application in Modeling and Numerical Approximations*, Springer, New York, 2005.
[21] D. Knees, *Global stress regularity of convex and some nonvex variational problems*, Ann. Mat. Pura Appl., 187 (2008), pp. 157–184.
[22] R. S. Laugesen and B. A. Siudeja, *Minimizing Neumann fundamental tones of triangles: An optimal Poincaré inequality*, J. Differential Equations, 249 (2010), pp. 118–135.
[23] L. D. Marini, *An inexpensive method for the evaluation of the solution of the lowest order Raviart-Thomas mixed method*, SIAM J. Numer. Anal., 22 (1985), pp. 493–496.
[24] C. Ortner and D. Praetorius, *on the convergence of adaptive nonconforming finite element methods for a class of convex variational problems*, SIAM J. Numer. Anal., 49 (2011), pp. 346–367.
[25] R. T. Rockafellar, *Convex Analysis*, Princeton University Press, Princeton, NJ, 1970.